Nuclear Symmetry Energy & the R-mode Instability of Neutron Stars

Isaac Vidaña
CFC, University of Coimbra

Pulsars & their environments

May 18th-21st Meudon, Paris Observatory

In this talk …

Discuss a couple of aspects of the nuclear symmetry energy:

- ✓ Role of the tensor force on the symmetry energy
- ✓ Role of the symmetry energy on the r-mode instability

For details see:

Phys. Rev. C 84, 062801 (R) (2011)

Eur. Phys. J. A 50 2 (2014) 13

Symmetry 2015, 7, 15-31

Phys. Rev. C 85, 045808 (2012)

Neutron-Rich Matter EoS

- Neutron-rich matter

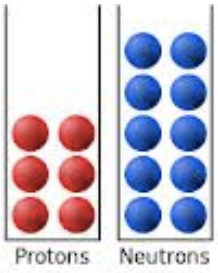

present in:

- ✓ Nuclei (especially far from stability line)
- ✓ Astrophysical systems (SN & NS)

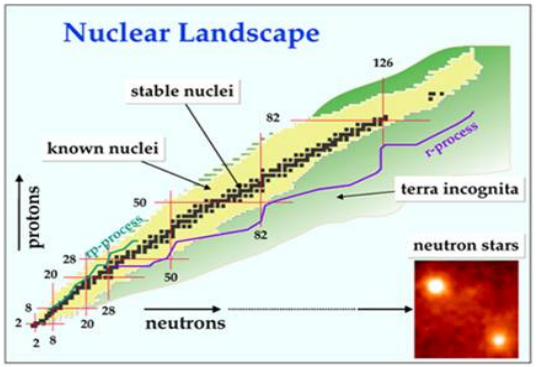

- Charge symmetry ➔ expansion of E/A on even powers of isospin asymmetry $\beta \approx (\rho_n - \rho_p)/(\rho_n + \rho_p)$

$$\frac{E}{A}(\rho,\beta) = E_{SNM}(\rho) + S_2(\rho)\beta^2 + S_4(\rho)\beta^4 + O(6)$$

$$E_{SNM}(\rho) = \frac{E}{A}(\rho,\beta=0), \qquad S_2(\rho) = \frac{1}{2}\frac{\partial^2 E/A}{\partial\beta^2}\bigg|_{\beta=0}, \qquad S_4(\rho) = \frac{1}{24}\frac{\partial^4 E/A}{\partial\beta^4}\bigg|_{\beta=0}$$

In good approximation:

$$S_2(\rho) \sim \frac{E}{A}(\rho,\beta=1) - \frac{E}{A}(\rho,\beta=0)$$

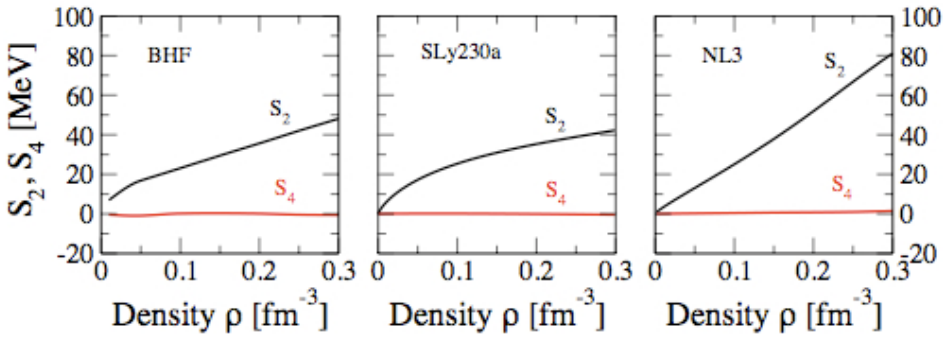

$E_{SNM}(\rho)$ commonly expanded around saturation density ρ_0

$$E_{SNM}(\rho) = E_0 + \frac{K_0}{2}\left(\frac{\rho-\rho_0}{3\rho_0}\right)^2 + \frac{Q_0}{6}\left(\frac{\rho-\rho_0}{3\rho_0}\right)^3 + O(4)$$

$$E_0 = E_{SNM}(\rho=\rho_0) \approx -16\,MeV$$

$$K_0 = 9\rho_0^2 \left.\frac{\partial^2 E_{SNM}(\rho)}{\partial\rho^2}\right|_{\rho=\rho_0} \approx 240 \pm 20\,MeV$$

$$Q_0 = 27\rho_0^3 \left.\frac{\partial^3 E_{SNM}(\rho)}{\partial\rho^3}\right|_{\rho=\rho_0} \approx -500 \div 300\,MeV$$

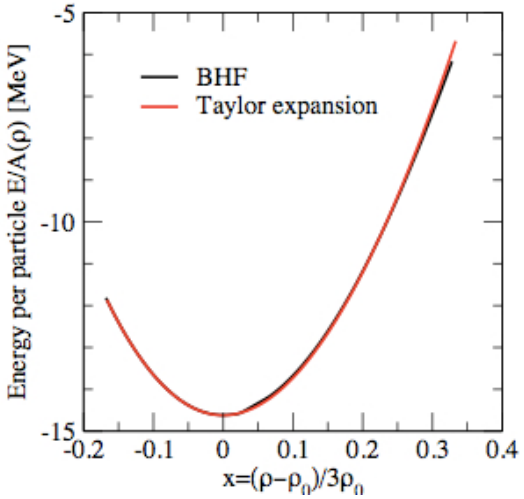

Similarly $S_2(\rho)$ can be also characterized with few bulk parameters around ρ_0

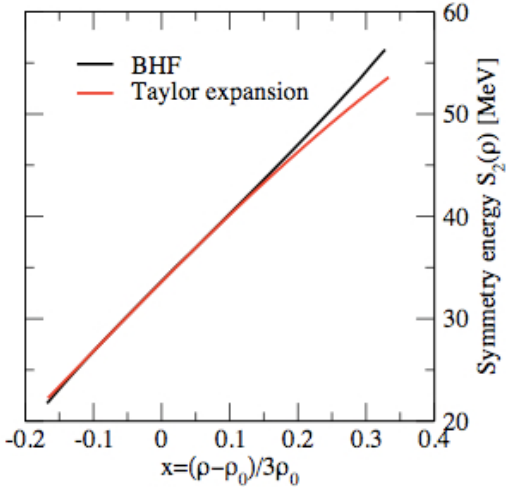

$$S_2(\rho) = E_{sym} + L\left(\frac{\rho-\rho_0}{3\rho_0}\right) + \frac{K_{sym}}{2}\left(\frac{\rho-\rho_0}{3\rho_0}\right)^2 + \frac{Q_{sym}}{6}\left(\frac{\rho-\rho_0}{3\rho_0}\right)^3 + O(4)$$

$$L = 3\rho_0 \left.\frac{\partial S_2(\rho)}{\partial\rho}\right|_{\rho=\rho_0} \quad K_{sym} = 9\rho_0^2 \left.\frac{\partial^2 S_2(\rho)}{\partial\rho^2}\right|_{\rho=\rho_0} \quad Q_{sym} = 27\rho_0^3 \left.\frac{\partial^3 S_2(\rho)}{\partial\rho^3}\right|_{\rho=\rho_0}$$

Less certain & predictions of different models vary largely

Different model predictions

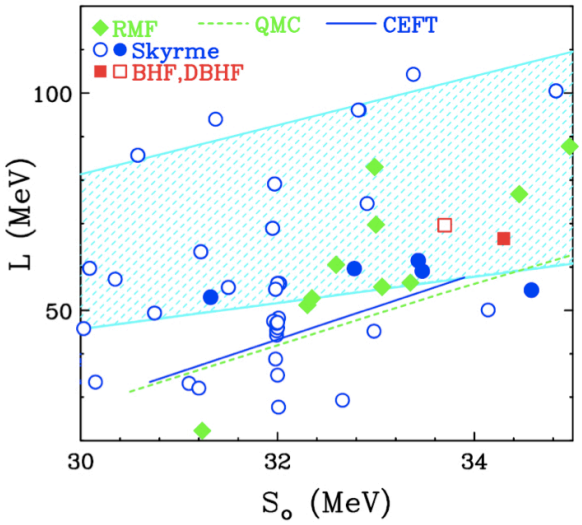

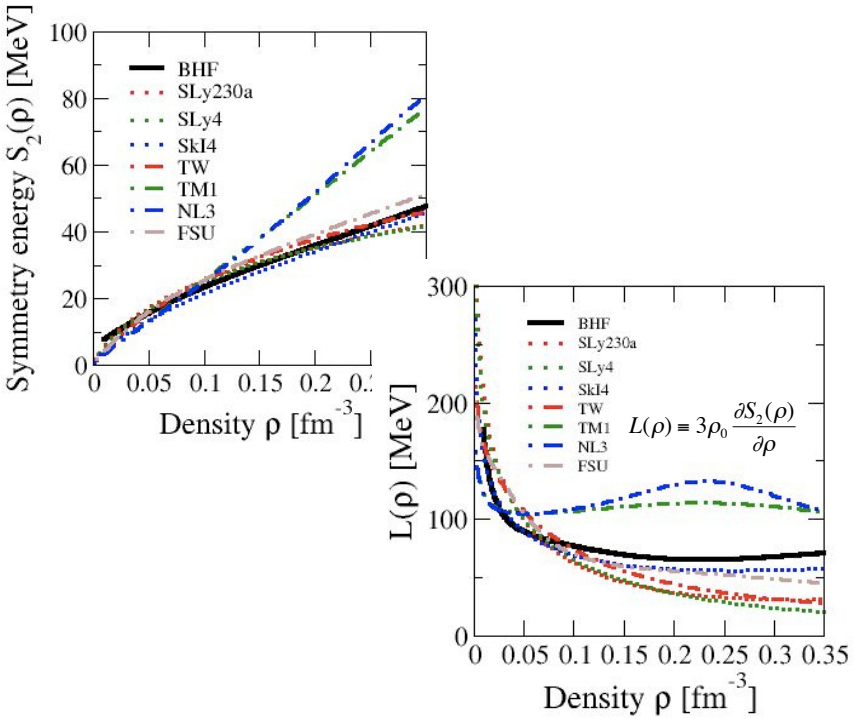

Model	ρ_0 (fm^{-3})	E_0 (MeV)	K_0 (MeV)	Q_0 (MeV)	J (MeV)	L (MeV)	K_{sym} (MeV)	Q_{sym} (MeV)
Microscopic								
BHF-1	0.187	−15.23	195.50	−280.90	34.30	66.55	−31.30	−112.80
Skyrme								
BSk14	0.159	−15.86	239.38	−358.78	30.00	43.91	−152.03	388.30
BSk16	0.159	−16.06	241.73	−363.69	30.00	34.87	−187.39	461.93
BSk17	0.159	−16.06	241.74	−363.73	30.00	36.28	−181.86	450.52
G_σ	0.158	−15.59	237.29	−348.82	31.37	94.02	13.99	−26.77
R_σ	0.158	−15.59	237.41	−348.50	30.58	85.70	−9.13	22.23
LNS	0.175	−15.32	210.83	−382.67	33.43	61.45	−127.37	302.48
NRAPR	0.161	−15.86	225.70	−362.65	32.78	59.63	−123.33	311.63
RATP	0.160	−16.05	239.58	−349.94	29.26	32.39	−191.25	440.74
SV	0.155	−16.05	305.75	−175.86	32.82	96.10	24.19	47.97
SGII	0.158	−15.60	214.70	−381.02	26.83	37.62	−145.92	330.44
SkI2	0.158	−15.78	240.99	−339.81	33.38	104.35	70.71	51.60
SkI3	0.158	−15.99	258.25	−303.96	34.83	100.53	73.07	211.53
SkI4	0.160	−15.95	247.98	−331.26	29.50	60.40	−40.52	351.09
SkI5	0.156	−15.85	255.85	−302.05	36.64	129.34	159.60	11.71
SkI6	0.159	−15.92	248.65	−327.44	30.09	59.70	−47.27	378.96
SkMP	0.157	−15.57	230.93	−338.15	29.89	70.31	−49.82	159.44
SkO	0.160	−15.84	223.39	−392.98	31.97	79.14	−43.17	131.12
Sly230a	0.160	−15.99	229.94	−364.29	31.98	44.31	−98.21	602.92
Sly230b	0.160	−15.98	229.96	−363.21	32.01	45.96	−119.72	521.54
SLy4	0.160	−15.98	229.97	−363.22	32.00	45.94	−119.74	521.58
SLy10	0.156	−15.91	229.74	−358.43	31.98	38.74	−142.19	591.28
Relativistic								
NL3	0.148	−16.24	270.70	188.80	37.34	118.30	100.50	182.60
TM1	0.145	−16.26	280.40	−295.40	36.84	110.60	33.55	−65.20
GM1	0.153	−16.32	299.70	−222.10	32.48	93.87	17.89	25.77
GM3	0.153	−16.32	239.90	−515.50	32.48	89.66	−6.47	55.86
FSU	0.148	−16.30	229.20	−537.40	32.54	60.40	−51.41	426.60
NL$\omega\rho$(025)	0.148	−16.24	270.70	188.80	32.35	61.05	−34.36	1322.00
TW	0.153	−16.25	240.20	−541.00	32.76	55.30	−124.70	539.00
DD-ME1	0.152	−16.23	244.50	307.60	33.06	55.42	−101.00	706.30
DD-ME2	0.152	−16.14	250.90	478.30	32.30	51.24	−87.19	777.10
DDHδI-25	0.153	−16.25	240.20	−540.30	25.62	48.56	81.10	928.30
DDHδII-30	0.153	−16.25	240.20	−540.30	31.89	57.52	80.74	1005.00
NL$\rho\delta$(2.5)	0.160	−16.05	240.40	−470.20	30.71	102.70	127.20	282.90
NL$\rho\delta$(1.7)	0.160	−16.05	240.40	−470.20	30.70	97.14	86.46	202.80
NL$\rho\delta$(0)	0.160	−16.05	240.40	−470.20	30.34	84.51	3.33	61.40

Some properties of asymmetric nuclear matter can be obtained from:

- the analysis of experimental data in heavy ion collisions
(e.g., ID, double n/p ratios, GDR, …)

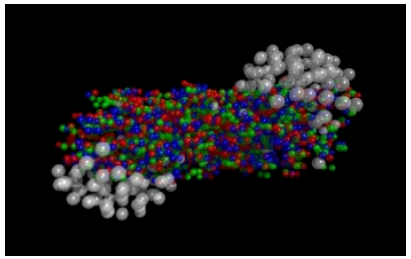

- the analysis of existing correlations between different quantities in bulk matter & finite nuclei
(e.g. δR versus L)

PREX, CREX experiment @ JLAB

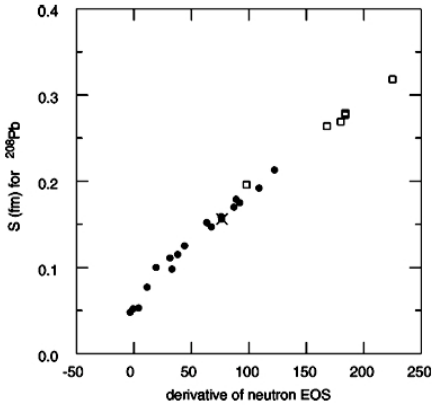

A major effort is being carried out to study experimentally the properties of asymmetric nuclear systems. Experiments at CSR , GSI (FAIR), RIKEN, GANIL, FRIB can probe the behavior of the symmetry energy close and above saturation density.

Astrophysical observations of compact objects
➔ window into nuclear matter at extreme isospin asymmetries

Symmetry Energy Sensitive Observables

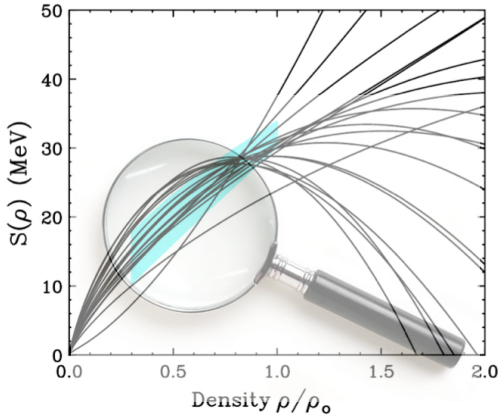

- Sub-saturation densities

✓ Neutron skin thickness in heavy nuclei
✓ Giant & pygmy resonances in neutron-rich nuclei
✓ n/p & $t/^3He$ ratios in nuclear reactions
✓ Isospin fragmentation & isospin scaling in nuclear multi-fragmentation
✓ Neutron-proton correlation functions at low relative momenta
✓ Isospin diffusion/transport in heavy ion collisions
✓ Neutron-proton differential flow

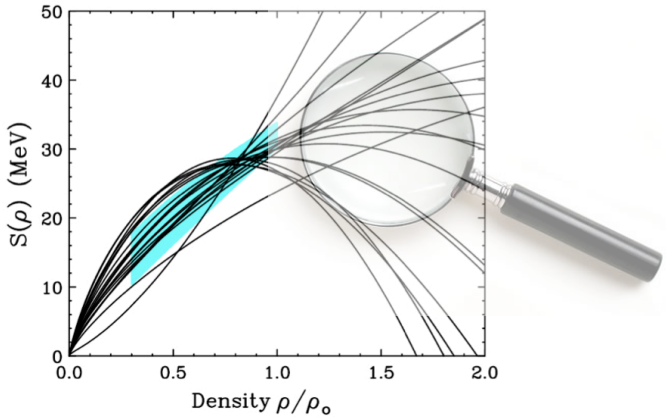

- Supra-saturation densities

✓ π^-/π^+ & K^-/K^+ ratios in heavy ion collisions
✓ Neutron-proton differential transverse flow
✓ n/p ratio of squeezed out nucleons perpendicular to the reaction plane
✓ Nucleon elliptic flow at high transverse momenta

Nevertheless, $E_{sym}(\rho)$ is still uncertain …

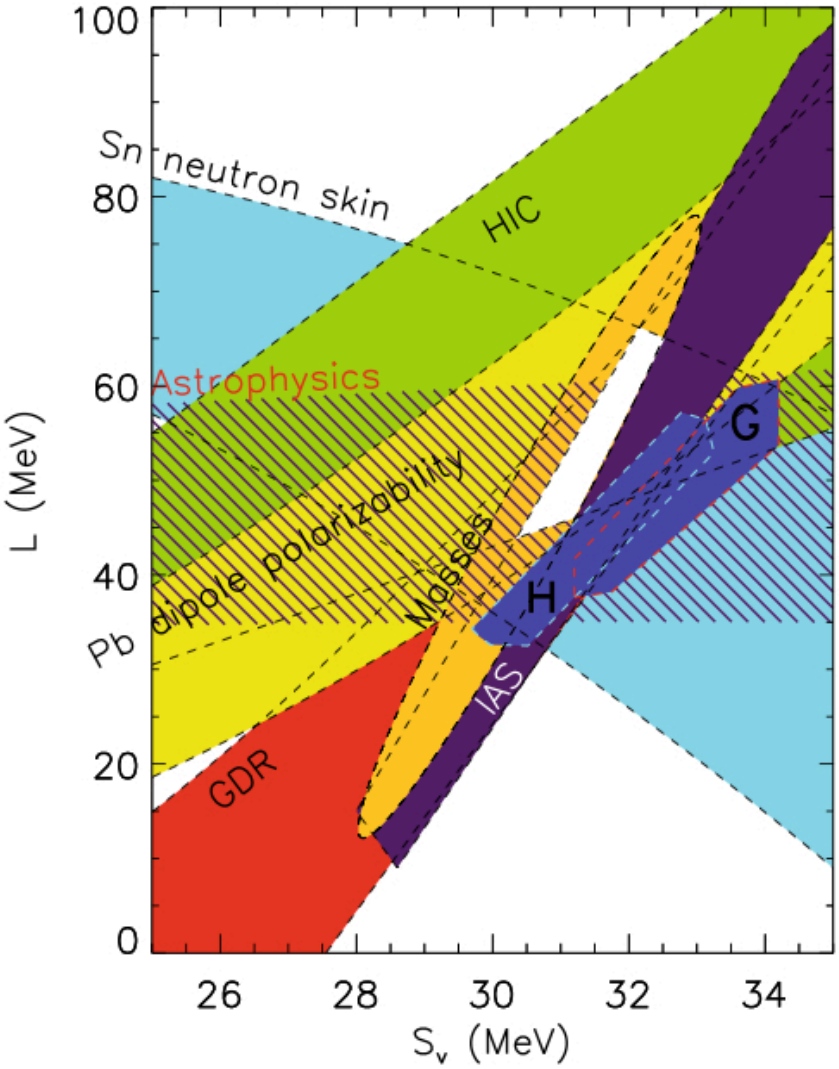

These two plots summarize our present knowledge or ignorance, if you prefer, on the symmetry energy & its density dependence

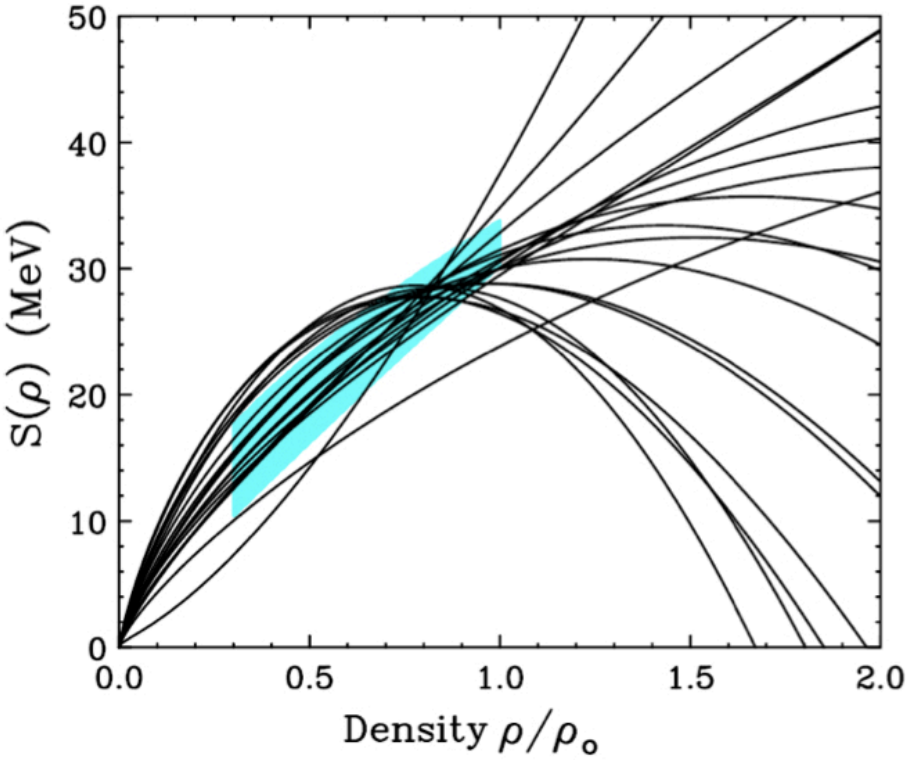

J. M. Lattimer & A. W. Steiner, EPJA 50, 40 (2014)

B. A. Brown, PRL 85, 5296 (2001)

Symmetry energy & role of the tensor force

Analysis of the contribution of the different terms of the NN force to E_{sym} & L using BHF (Av18+UIX) + Hellman-Feynman theorem

In collaboration with a couple of people you know:

Constança Providência

Artur Polls

Phys. Rev. C 84, 062801 (R) (2011)

BHF approximation in a nutshell

✧ Energy per particle

- $$\frac{E}{A}(\rho,\beta) = \underbrace{\frac{1}{A}\sum_{\tau}\sum_{k\le k_{F_\tau}}\frac{\hbar^2 k^2}{2m_\tau}}_{\text{Free Fermi Gas}} + \underbrace{\frac{1}{2A}\sum_{\tau}\sum_{k\le k_{F_\tau}}\mathrm{Re}\left[U_\tau(\vec{k})\right]}_{\text{Correlation Energy}}$$

Infinite sumation of two-hole line diagrams

✧ Bethe-Goldstone Equation

- $$G(\omega) = V + V\frac{Q}{\omega - E - E' + i\eta}G(\omega)$$
- $$E_\tau(k) = \frac{\hbar^2 k^2}{2m_\tau} + \mathrm{Re}\left[U_\tau(k)\right]$$
- $$U_\tau(k) = \sum_{\tau'}\sum_{k'\le k_{F_{\tau'}}}\left\langle \vec{k}\vec{k}' \left| G\left(\omega = E_\tau(k) + E_{\tau'}(k')\right) \right| \vec{k}\vec{k}' \right\rangle_{\mathcal{A}}$$

Partial sumation of pp ladder diagrams

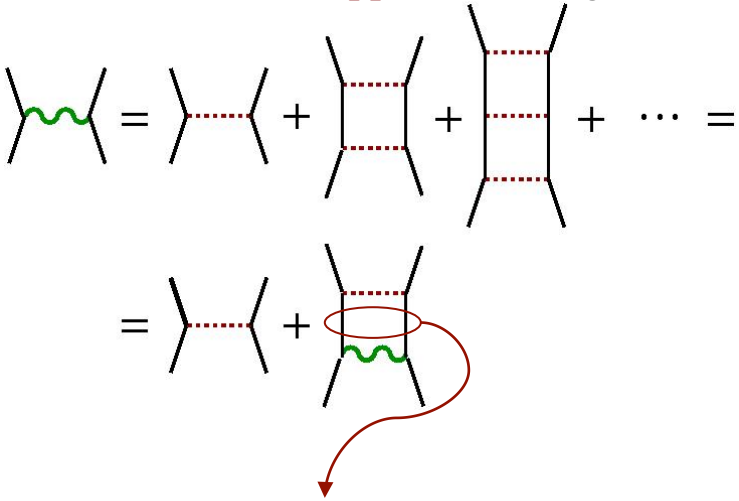

- ✓ Pauli blocking
- ✓ Nucleon dressing

BHF nucleon mean field

$$U_\tau(k) = \sum_{\tau'} \sum_{k' \le k_{F_{\tau'}}} \left\langle \vec{k}\vec{k}' \middle| G\left(\omega = E_\tau(k) + E_{\tau'}(k')\right) \middle| \vec{k}\vec{k}' \right\rangle_A$$

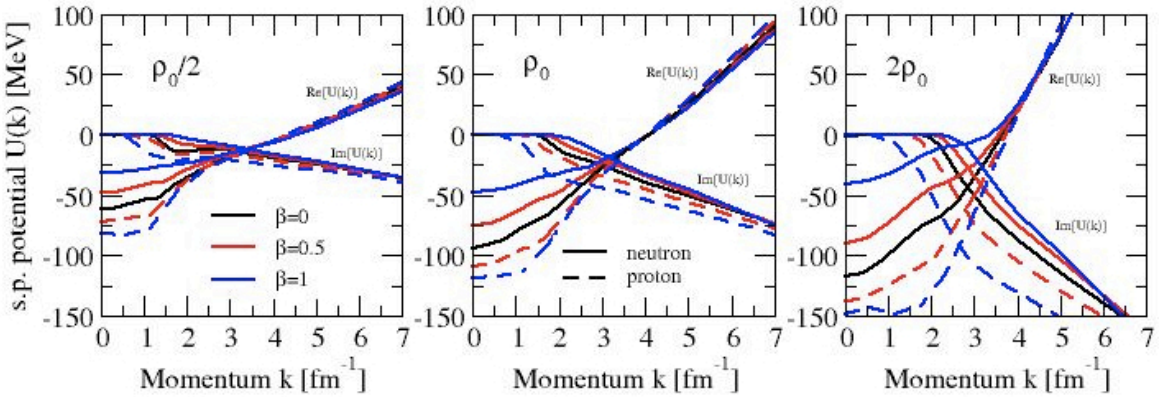

Isospin splitting of mean field in ANM

$$U_n \sim U_0 + U_{sym}\beta$$

$$U_p \sim U_0 - U_{sym}\beta$$

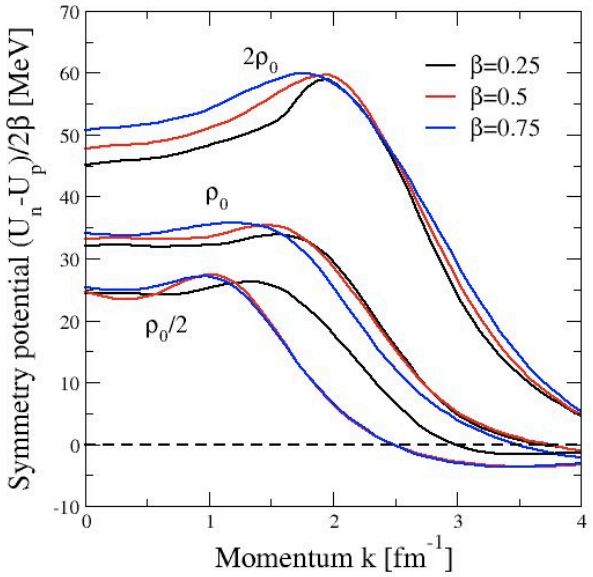

Symmetry potential

$$U_{sym} = \frac{U_n - U_p}{2\beta}$$

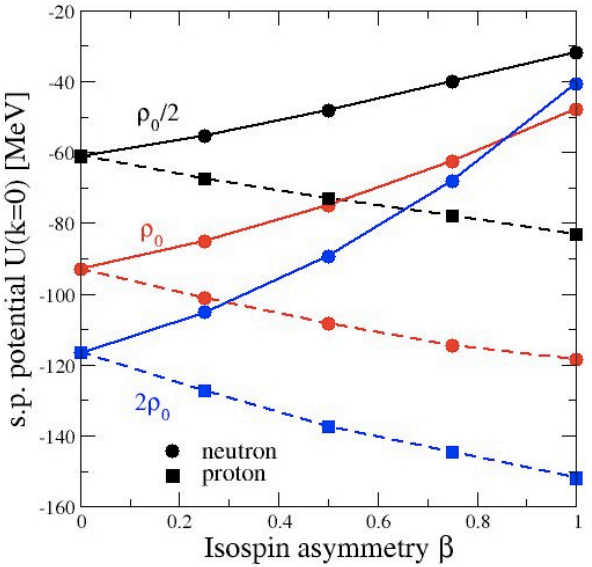

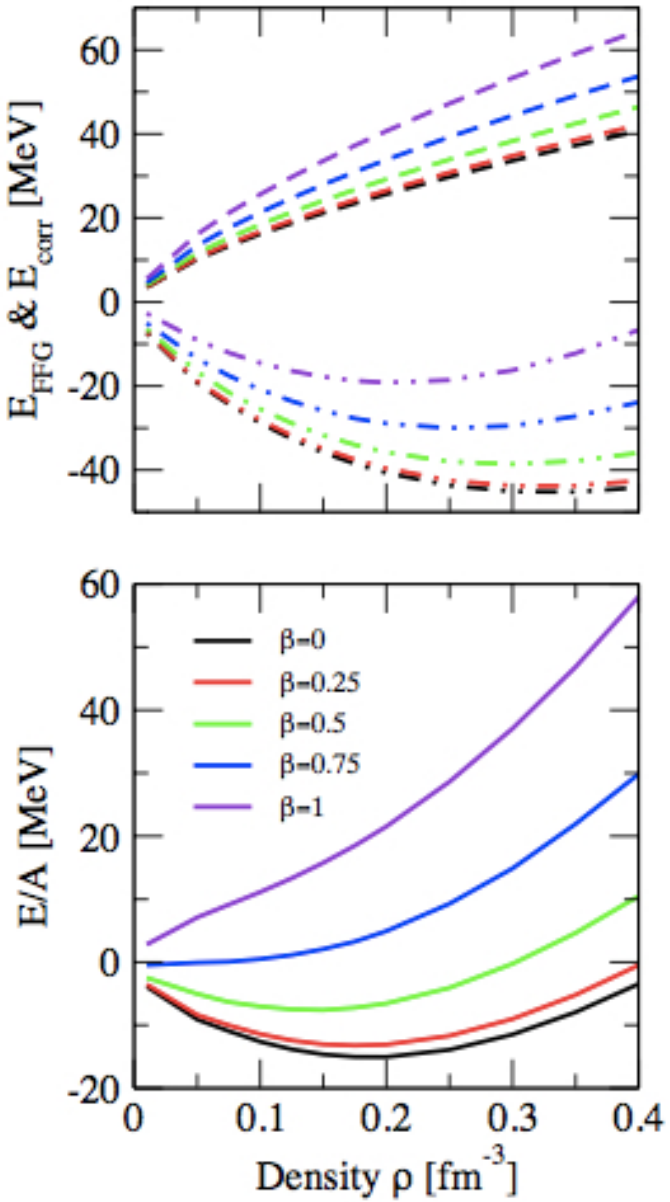

(BHF with Av18+UIX)

Brueckner-Hatree-Fock:

✓ Provides separately E_{FFG} & E_{Corr}

But

✓ does not gives separately neither <T> nor <V> because it does not provide the correlated many-body wave function

However

Hellmann-Feynman theorem can be used to calculate <V> and then <T> from E - <V>

Hellmann-Feynman theorem

Proven independently by many-authors:
Güttinger (1932), Pauli (1933), Hellmann (1937), Feynman (1939)

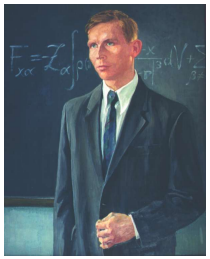

H. Hellmann

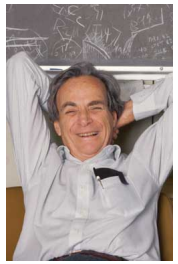

R. P. Feynman

$$\frac{dE_\lambda}{d\lambda} = \frac{\langle \psi_\lambda | \frac{d\hat{H}_\lambda}{d\lambda} | \psi_\lambda \rangle}{\langle \psi_\lambda | \psi_\lambda \rangle}$$

- Writing the nuclear matter Hamiltonian as: $\hat{H} = \hat{T} + \hat{V}$
- Defining a λ-dependent Hamiltonian: $\hat{H}_\lambda = \hat{T} + \lambda \hat{V}$

$$\Rightarrow \quad \langle \hat{V} \rangle = \frac{\langle \psi | \hat{V} | \psi \rangle}{\langle \psi | \psi \rangle} = \left(\frac{dE_\lambda}{d\lambda} \right)\Bigg|_{\lambda=1}$$

Kinetic and Potential Energy Contributions

Contribution	E_{PNM}	E_{SNM}	E_{sym}	L
$\langle T \rangle$	53.321	54.294	−0.973	14.896
$\langle V \rangle$	−34.251	−69.524	35.273	51.604
Total	19.070	−15.230	34.300	66.500

(BHF Av18+UIX saturation point ρ_0=0.187 fm^{-3})

- Potential energy contribution

✓ E_{sym}: almost equal to total E_{sym} in all the density range

✓ L: ~ 78% of the total L

- Kinetic energy contribution

✓ E_{sym}: very small in the whole density range and negative below ~ 0.2 fm^{-3} in contrast to FFG result (~ 14 MeV at ρ_0)

➔ strong isospin dependence of short range NN correlations (Xu & Li (2011), I.V., et al., (2011), Carbone et al., (2012), Hen et al., (2015), Cai & Li (2015))

✓ L: smaller than FFG (~ 29 MeV at ρ_0) one in the full density range

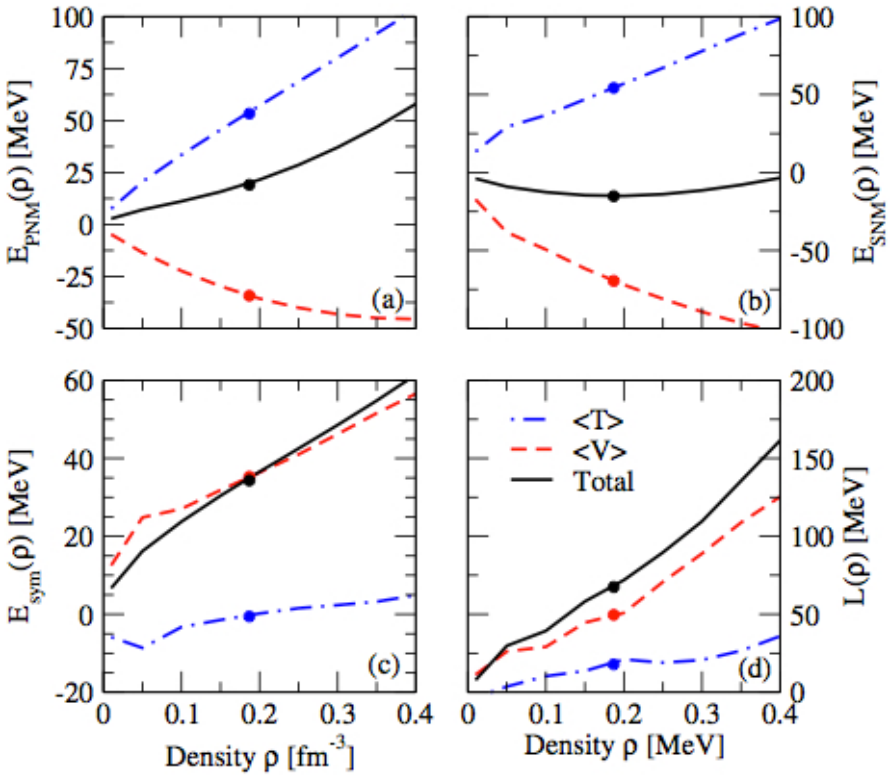

Kinetic Energy of Correlated & Uncorrelated Systems

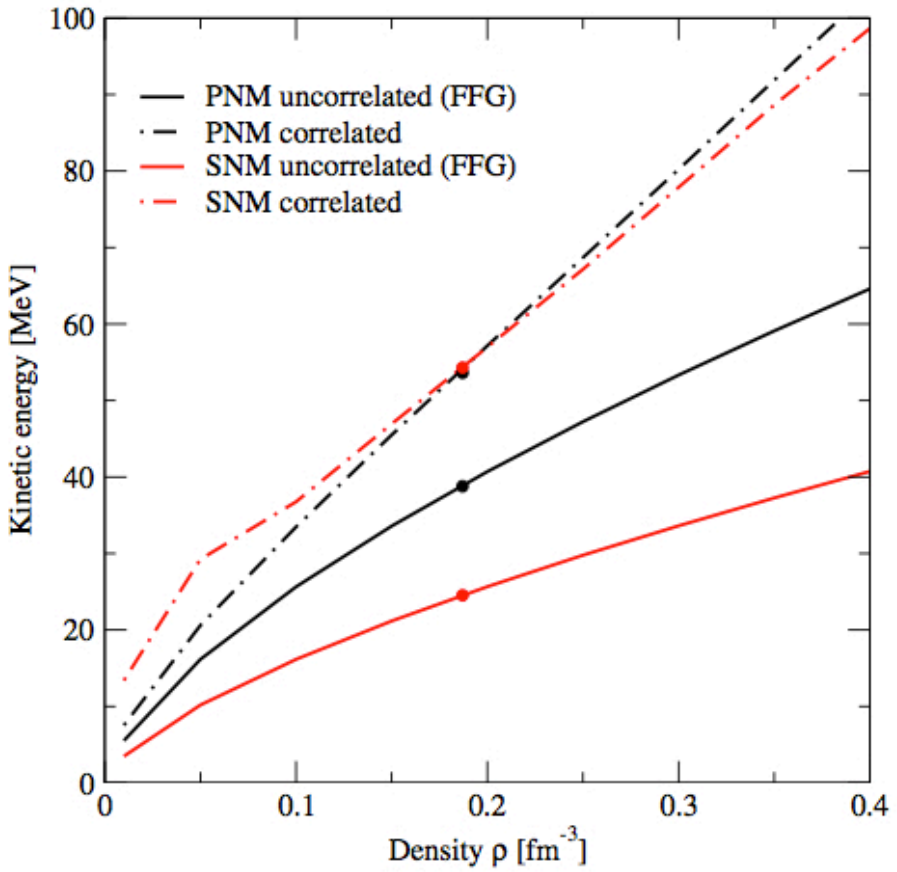

✓ Increase of kinetic energy of SNM due to SRC is always much larger than that of PNM

✓ Kinetic energy of both correlated systems (SNM & PNM) is of similar order. Their strong cancellation leads to the small contribution to E_{sym}

In agreement with:

- Xu & Li (2011) Hen et al., (2015): phenomenological n(k)
- Carbone et al., (2012): SCGF with Av18 & CDBONN
- Cai & Li (2015): RMF with HMT

Spin-Isospin Channel & Partial Wave Decomposition

(S,T)	$\langle V\rangle_{PNM}$	$\langle V\rangle_{SNM}$	$E^{sym}_{\langle V\rangle}$	$L_{\langle V\rangle}$
$(0,0)$	0	5.600	−5.600	−21.457
$(0,1)$	−29.889	−23.064	−6.825	−17.950
$(1,0)$	0	−49.836	49.836	90.561
$(1,1)$	−4.3621	−2.224	−2.138	0.450

- ✓ Largest contribution from S=1, T=0 channel
- ✓ Similar T=1 channel contributions to $\langle V\rangle_{PNM}$ and $\langle V\rangle_{SNM}$ which almost cancel out in $E_{\langle v\rangle}^{sym}$
- ✓ Main contribution from $^3S_1$-$^3D_1$ p.w. (not present in NM)

Partial Wave	$\langle V\rangle_{PNM}$	$\langle V\rangle_{SNM}$	$E^{sym}_{\langle V\rangle}$	$L_{\langle V\rangle}$
$^1S_0$	−23.070	−19.660	−3.410	−3.459
$^3S_1$	0	−45.810	45.810	71.855
$^1P_1$	0	4.904	−4.904	−18.601
$^3P_0$	−5.321	−4.029	−1.292	−1.898
$^3P_1$	16.110	10.720	5.390	21.949
$^3P_2$	−16.000	−9.334	−6.666	−21.168
$^1D_2$	−5.956	−3.201	−2.755	−11.033
$^3D_1$	0	0.981	−0.981	−3.739
$^3D_2$	0	−3.982	3.982	16.601
$^3D_3$	0	−0.798	0.798	4.895
$^1F_3$	0	0.694	−0.694	−3.348
$^3F_2$	−0.695	−0.229	−0.466	−1.799
$^3F_3$	2.000	0.821	1.179	4.883
$^3F_4$	−0.796	−0.194	−0.602	−3.239
$^1G_4$	−0.812	−0.247	−0.565	−3.036
$^3G_3$	0	−0.001	0.001	0.441
$^3G_4$	0	−0.213	0.213	0.449
$^3G_5$	0	−0.057	0.057	0.650
$^1H_5$	0	0.029	−0.029	0.107
$^3H_4$	0.033	0.040	−0.007	0.232
$^3H_5$	0.225	−0.033	0.258	0.968
$^3H_6$	0.043	0.034	0.009	0.144
Rest up to $J=8$	−0.012	0.041	−0.161	−0.250

(BHF Av18+UIX saturation point ρ_0=0.187 fm^{-3})

Few words on the NN and NNN forces used …

- **Argonne V18 (Av18) NN potential**

$$V_{ij} = \sum_{p=1,18} V_p(r_{ij}) O_{ij}^p$$

$$O_{ij}^{p=1,14} = \left[1, (\vec{\sigma}_i \cdot \vec{\sigma}_j), S_{ij}, \vec{L}\cdot\vec{S}, L^2, L^2(\vec{\sigma}_i \cdot \vec{\sigma}_j), (\vec{L}\cdot\vec{S})^2\right] \otimes \left[1, (\vec{\tau}_i \cdot \vec{\tau}_j)\right]$$

$$O_{ij}^{p=15,18} = \left[T_{ij}, (\vec{\sigma}_i \cdot \vec{\sigma}_j) T_{ij}, S_{ij} T_{ij}, (\tau_{zi} + \tau_{zj})\right]$$

- **Urbana IX (UIX) NNN potential**

$$V_{ijk}^{UIX} = V_{ijk}^{2\pi} + V_{ijk}^{R}$$

$V_{ijk}^{2\pi}$: Attractive Fujita-Miyazawa force

$$V_{ijk}^{2\pi} = A \sum_{cyclic} \left(\{X_{ij}, X_{jk}\} \{\vec{\tau}_i \cdot \vec{\tau}_j, \vec{\tau}_j \cdot \vec{\tau}_k\} + \frac{1}{4} [X_{ij}, X_{jk}][\vec{\tau}_i \cdot \vec{\tau}_j, \vec{\tau}_j \cdot \vec{\tau}_k] \right)$$

$$X_{ij} = Y(m_\pi r_{ij}) \vec{\sigma}_i \cdot \vec{\sigma}_j + T(m_\pi r_{ij}) S_{ij}$$

$$Y(x) = \frac{e^{-x}}{x}\left(1 - e^{x^2}\right) \qquad T(x) = \left(1 + \frac{3}{x} + \frac{3}{x^2}\right)\frac{e^{-x}}{x}\left(1 - e^{x^2}\right)^2$$

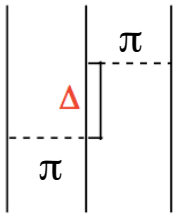

V_{ijk}^{R} : Repulsine & Phenomenological

$$V_{ijk}^{R} = B \sum_{cyclic} T^2(r_{ij}) T^2(r_{jk})$$

Reduced to an effective density-dependent 2BF

$$U_{NN}^{eff}(\vec{r}_{ij}) = \int V^{UIX}(\vec{r}_i, \vec{r}_j, \vec{r}_k) n(\vec{r}_i, \vec{r}_j, \vec{r}_k) d^3\vec{r}_k \longrightarrow O_{ij}^{p=1,3} = 1, (\vec{\sigma}_i \cdot \vec{\sigma}_j)(\vec{\tau}_i \cdot \vec{\tau}_j), S_{ij}(\vec{\tau}_i \cdot \vec{\tau}_j)$$

Contributions from different terms of the NN force

Component	$\langle V \rangle_{PNM}$	$\langle V \rangle_{SNM}$	$E^{sym}_{\langle V \rangle}$	$L_{\langle V \rangle}$
$\langle V_1 \rangle$	−31.212	−32.710	1.498	−5.580
$\langle V_{\vec{\tau}_i \cdot \vec{\tau}_j} \rangle$	−4.957	3.997	−8.954	−20.383
$\langle V_{\vec{\sigma}_i \cdot \vec{\sigma}_j} \rangle$	−0.319	−0.382	0.063	2.392
$\langle V_{(\vec{\sigma}_i \cdot \vec{\sigma}_j)(\vec{\tau}_i \cdot \vec{\tau}_j)} \rangle$	−5.724	−11.388	5.664	2.521
$\langle V_{S_{ij}} \rangle$	−0.792	1.912	−2.704	−4.998
$\langle V_{S_{ij}(\vec{\tau}_i \cdot \vec{\tau}_j)} \rangle$	−4.989	−37.592	32.603	47.095
$\langle V_{\vec{L} \cdot \vec{S}} \rangle$	−7.538	−1.754	−5.784	−12.251
$\langle V_{\vec{L} \cdot \vec{S}(\vec{\tau}_i \cdot \vec{\tau}_j)} \rangle$	−2.671	−6.539	3.868	3.969
$\langle V_{L^2} \rangle$	11.850	13.610	−1.760	1.521
$\langle V_{L^2(\vec{\tau}_i \cdot \vec{\tau}_j)} \rangle$	−2.788	0.270	−3.058	−14.262
$\langle V_{L^2(\vec{\sigma}_i \cdot \vec{\sigma}_j)} \rangle$	1.265	1.383	−0.118	1.405
$\langle V_{L^2(\vec{\sigma}_i \cdot \vec{\sigma}_j)(\vec{\tau}_i \cdot \vec{\tau}_j)} \rangle$	0.051	0.008	0.043	−0.341
$\langle V_{(\vec{L} \cdot \vec{S})^2} \rangle$	4.194	5.682	−1.488	−0.327
$\langle V_{(\vec{L} \cdot \vec{S})^2(\vec{\tau}_i \cdot \vec{\tau}_j)} \rangle$	5.169	−6.190	11.359	31.368
$\langle V_{T_{ij}} \rangle$	0.003	0.039	−0.036	−0.022
$\langle V_{(\vec{\sigma}_i \cdot \vec{\sigma}_j)T_{ij}} \rangle$	−0.017	−0.106	0.089	0.042
$\langle V_{S_{ij}T_{ij}} \rangle$	0.004	0.079	−0.075	−0.124
$\langle V_{(\tau_{z_i} + \tau_{z_j})} \rangle$	−0.084	−0.001	−0.083	−0.331
$\langle U_1 \rangle$	2.985	3.251	−0.266	−0.630
$\langle U_{(\vec{\sigma}_i \cdot \vec{\sigma}_j)(\vec{\tau}_i \cdot \vec{\tau}_j)} \rangle$	2.254	3.999	−1.745	−7.228
$\langle U_{S_{ij}(\vec{\tau}_i \cdot \vec{\tau}_j)} \rangle$	−0.935	−7.092	6.157	27.768

(BHF Av18+UIX saturation point ρ_0=0.187 fm^{-3})

✓ Largest contribution from tensor components

- E_{sym}: 36.056 (Total: 34.4)
- L: 69.968 (Total: 66.5)

✓ Contributions from other terms negligible (e.g. charge symmetry breaking terms) or almost cancel out

➔ Tensor force dominates both E_{sym} & L

Role of the symmetry energy on the r-mode instability

Study the role of the symmetry energy slope parameter L on the r-mode instability of neutron stars by using both microscopic (BHF, APR & AFDMC) and phenomenological (Skyrme & RMF) approaches of the nuclear matter EoS

Phys. Rev. C 85, 045808 (2012)

The r-mode instability in another nutshell

Ω_{Kepler} : Absolute Upper Limit of Rot. Freq.

Instabilities prevent NS to reach Ω_{Kepler}

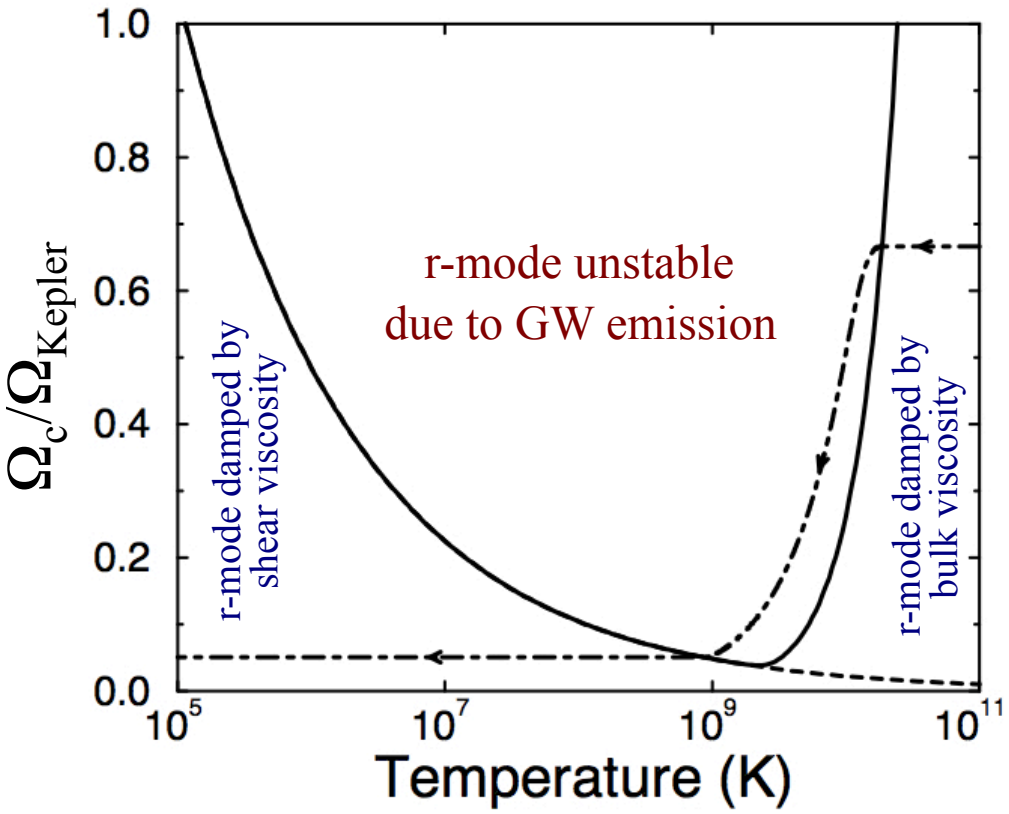

r-mode instability : toroidal mode of oscillation

✓ restoring force: Coriolis

✓ emission of GW (CFS mechanism)

- GW makes the mode unstable
- Viscosity stabilizes the mode

$$A \propto A_0 e^{-i\omega(\Omega)-t/\tau(\Omega,T)}$$

$$\frac{1}{\tau(\Omega,T)} = -\frac{1}{\tau_{GW}(\Omega)} + \frac{1}{\tau_{Viscosity}(\Omega,T)}$$

Bulk & shear viscosities

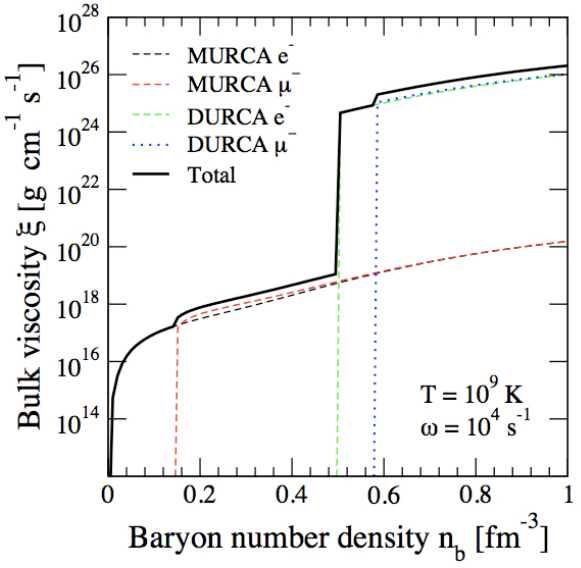

$$\xi = \xi_{MURCA} + \xi_{DURCA} = \sum_{Nl} \frac{|\lambda_{Nl}|}{\omega^2} \left|\frac{\partial P}{\partial X_l}\right| \frac{\partial \varsigma_l}{\partial n_b} + \sum_{l} \frac{|\lambda_{l}|}{\omega^2} \left|\frac{\partial P}{\partial X_l}\right| \frac{\partial \varsigma_l}{\partial n_b}$$

✓ Modified URCA

$$N + n \rightarrow N + p + l + \bar{\nu}_l, \qquad N + p + l \rightarrow N + n + \nu_l$$

✓ Direct URCA

$$n \rightarrow p + l + \bar{\nu}_l, \qquad p + l \rightarrow n + \nu_l$$

Haensel et al., AA 357, 1157 (2000); AA 372, 130 (2001)

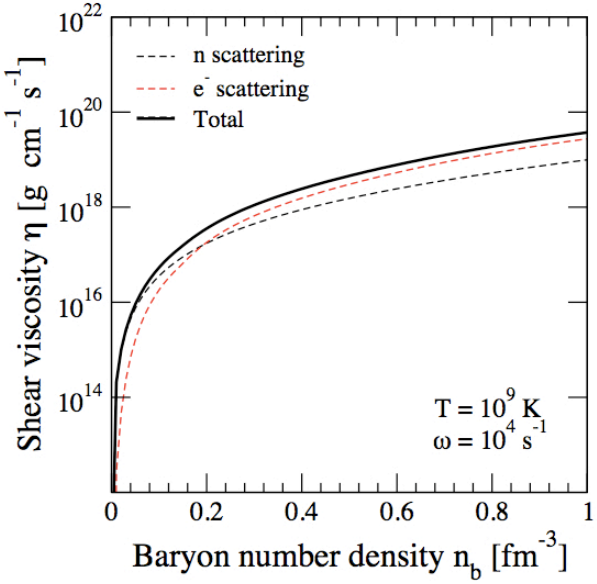

$$\eta = \eta_n + \eta_e$$

✓ n scattering [1]

$$\eta_n = 2 \times 10^{18} \left(\frac{\rho}{10^{15}\, g cm^{-3}}\right)^{9/4} \left(\frac{T}{10^9 K}\right)^{-2}$$

✓ e⁻ scattering [2]

$$\eta_e = 4.26 \times 10^{-26} \left(x_p n_b\right)^{14/9} T^{-5/3}$$

[1] Cutler & Lindblom., ApJ 314, 234 (1987)
[2] Shternin & Yakovlev, PRD 78, 063006 (2008)

L dependence of ξ and η

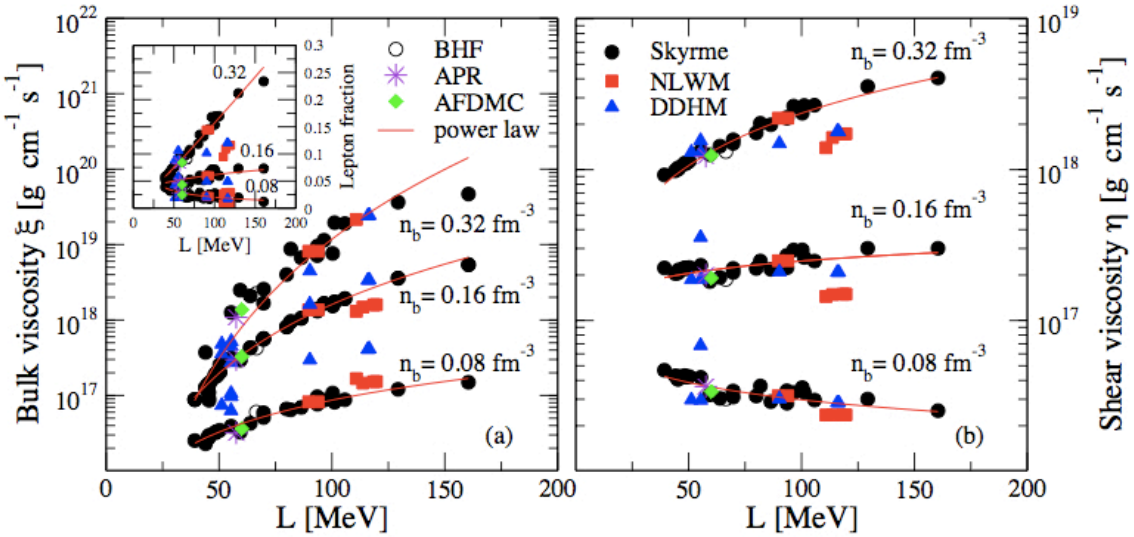

- ✓ ξ increases with L for all densities
- ✓ η increases with L for $n_b > n_0$ & decreases with L for $n_b < n_0$

consequence of lepton fraction dependence

L dependence described by simple power laws

$$\xi = A_\xi L^{B_\xi}, \eta = A_\eta L^{B_\eta}$$

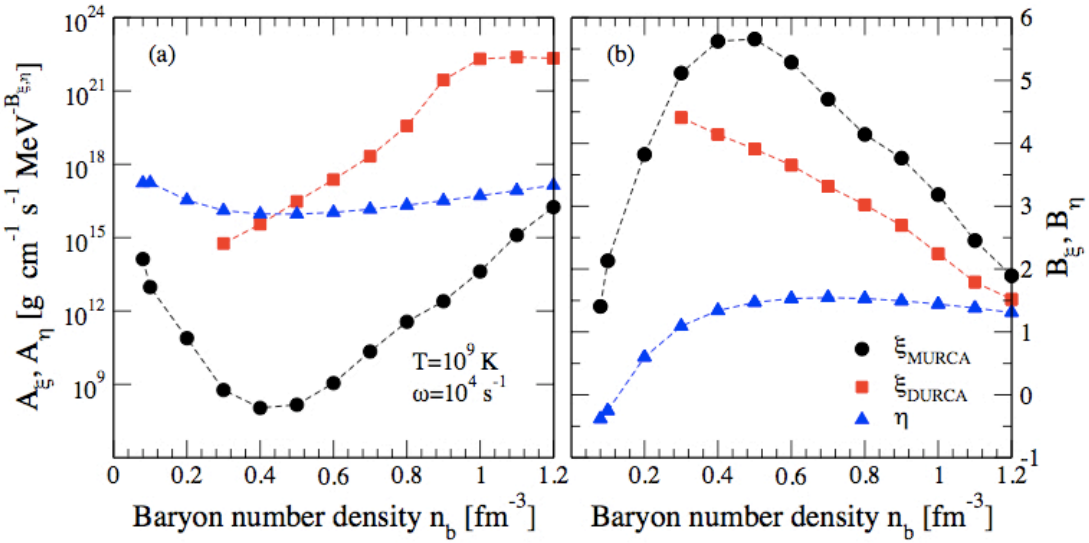

Dissipative time scales of r-modes

$$\frac{1}{\tau_i} = -\frac{1}{2E}\left(\frac{dE}{dt}\right)_i$$

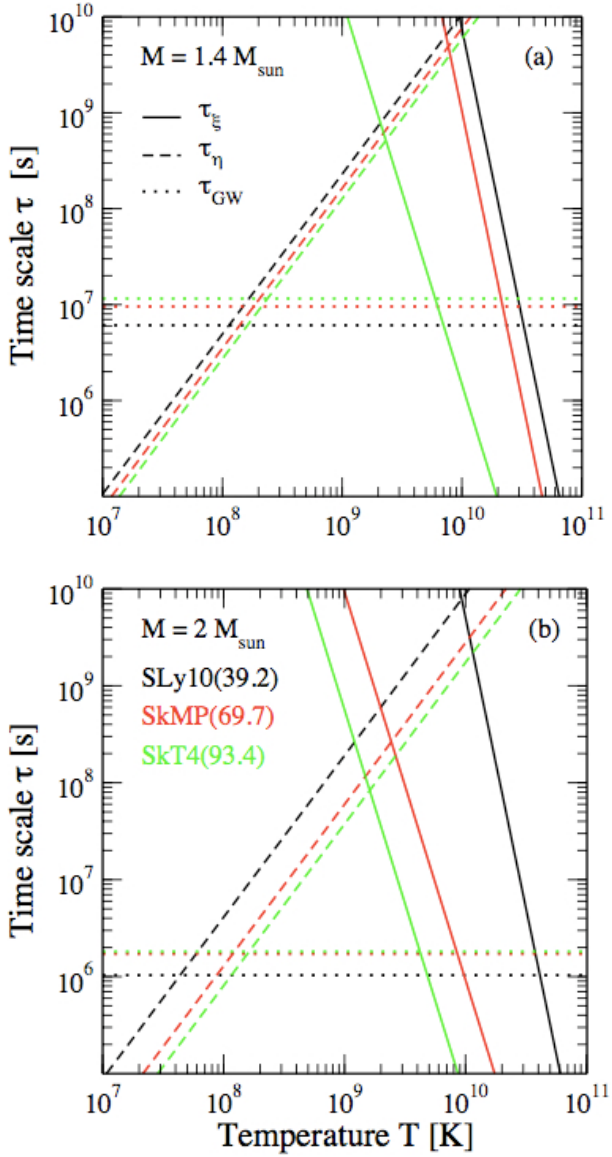

- $\frac{1}{\tau_\xi} = \frac{4\pi}{690}\left(\frac{\Omega^2}{\pi G\bar{\rho}}\right)^2 R^{2l-2}\left[\int_0^R \rho r^{2l+2}dr\right]^{-1}\int_0^R \xi\left(\frac{r}{R}\right)^2\left[1+0.86\left(\frac{r}{R}\right)^2\right]r^2dr$
- $\frac{1}{\tau_\eta} = (l-1)(2l+1)\left[\int_0^R \rho r^{2l+2}dr\right]^{-1}\int_0^R \eta r^{2l}dr$
- $\frac{1}{\tau_{GW}} = \frac{32\pi G\Omega^{2l+2}}{c^{2l+3}}\frac{(l-1)^{2l}}{[(2l+1)!!]^2}\left(\frac{l+2}{l+1}\right)^{2l+1}\int_0^R \rho r^{2l+2}dr$

✓ τ_{GW} larger for models with larger L

Larger L ➔ stiffer EoS ➔ less compact star ➔ τ_{GW} larger

✓ τ_ξ & τ_η smaller for models with larger L

τ_ξ (τ_η) decrease with $\xi(\eta)$ but $\xi(\eta)$ increase with L

✓ τ_{GW}, τ_ξ & τ_η decrease when increasing M

Given an EoS: the more massive the star the denser it is

➔ τ_{GW}, $\tau_\xi \sim (\rho/\xi)R^2$ & $\tau_\eta \sim (\rho/\eta)R^2$ decrease

R-mode instability region

- time dependence of an r-mode $\sim e^{i\omega t - t/\tau}$

$$\frac{1}{\tau(\Omega,T)} = -\frac{1}{\tau_{GW}(\Omega)} + \frac{1}{\tau_{\xi}(\Omega,T)} + \frac{1}{\tau_{\eta}(T)}$$

➔ $\frac{1}{\tau(\Omega_c,T)} = 0$ r-mode instability region

$\Omega < \Omega_c$ stable

$\Omega > \Omega_c$ unstable

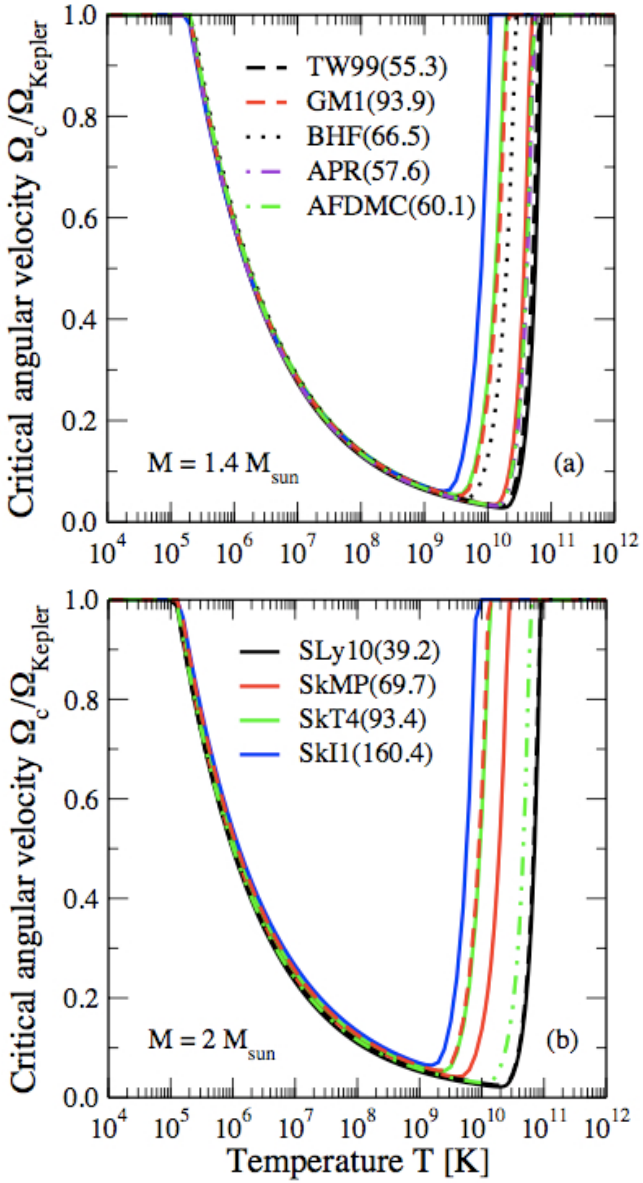

✓ instability region smaller for models with larger L (increase of ξ & η with L)

✓ instability region larger for more massive star (time scales decrease when M increases)

Constraining L from LMXB

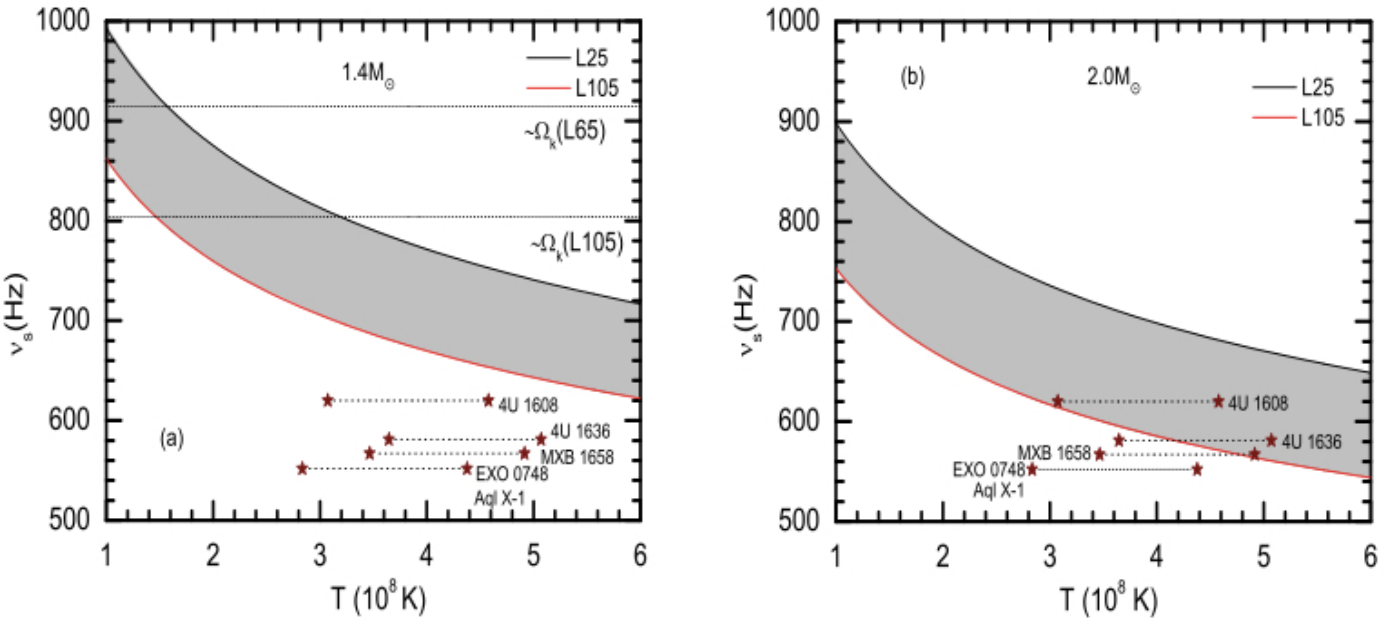

Using electron-electron scattering at the crust-core ($\rho<r_0$) boundary as the main dissipation mechanism Wen, Newton & Li obtained L < 60 MeV

Phys. Rev. C 85, 025801 (2012)

The final message of this talk

- The tensor force plays a critical role in the determation of E_{sym} & L
- The r-mode instability region is very sensitive to the symmetry energy: is smaller for models with larger L (increase of with ξ & η L). L dependence of ξ & η can be described by simple power laws $\xi=A_{\xi}L^{B\xi}$ & $\eta=A_{\eta}L^{B\eta}$.
- Constraints from LMXB seems to indicate L < 60 MeV

- You for your time & attention
- The organizers for their invitation
- COST for its support